JOURNAL OF BACTERIOLOGY, Jan. 2006, p. 202–210 Vol. 188, No. 1
0021-9193/06/$08.00+0 doi:10.1128/JB.188.1.202–210.2006

Reconstruction and Regulation of the Central Catabolic Pathway in the Thermophilic Propionate-Oxidizing Syntroph *Pelotomaculum thermopropionicum*

Tomoyuki Kosaka,[1] Taku Uchiyama,[1] Shun-ichi Ishii,[1] Miho Enoki,[1,2] Hiroyuki Imachi,[3] Yoichi Kamagata,[2] Akiyoshi Ohashi,[3] Hideki Harada,[3] Hiroshi Ikenaga,[1] and Kazuya Watanabe[1]*

Laboratory of Applied Microbiology, Marine Biotechnology Institute, Kamaishi, Iwate 026-0001,[1] National Institute of Bioscience and Human-Technology, Agency of Industrial Science and Technology, Tsukuba, Ibaraki 305-8566,[2] and Department of Environmental Systems Engineering, Nagaoka University of Technology, Nagaoka, Niigata 940-2188,[3] Japan

Received 31 August 2005/Accepted 17 October 2005

Obligate anaerobic bacteria fermenting volatile fatty acids in syntrophic association with methanogenic archaea share the intermediate bottleneck step in organic-matter decomposition. These organisms (called syntrophs) are biologically significant in terms of their growth at the thermodynamic limit and are considered to be the ideal model to address bioenergetic concepts. We conducted genomic and proteomic analyses of the thermophilic propionate-oxidizing syntroph *Pelotomaculum thermopropionicum* to obtain the genetic basis for its central catabolic pathway. Draft sequencing and subsequent targeted gap closing identified all genes necessary for reconstructing its propionate-oxidizing pathway (i.e., methylmalonyl coenzyme A pathway). Characteristics of this pathway include the following. (i) The initial two steps are linked to later steps via transferases. (ii) Each of the last three steps can be catalyzed by two different types of enzymes. It was also revealed that many genes for the propionate-oxidizing pathway, except for those for propionate coenzyme A transferase and succinate dehydrogenase, were present in an operon-like cluster and accompanied by multiple promoter sequences and a putative gene for a transcriptional regulator. Proteomic analysis showed that enzymes in this pathway were up-regulated when grown on propionate; of these enzymes, regulation of fumarase was the most stringent. We discuss this tendency of expression regulation based on the genetic organization of the open reading frame cluster. Results suggest that fumarase is the central metabolic switch controlling the metabolic flow and energy conservation in this syntroph.

Methane fermentation is a complex microbiological process and involves metabolic interactions among a variety of microorganisms. These microorganisms are classified into at least four trophic groups, namely, primary fermenting bacteria, secondary fermenting bacteria, hydrogenotrophic methanogenic archaea, and acetoclastic methanogenic archaea (39). Among these microorganisms, secondary fermenting bacteria oxidize volatile fatty acids and alcohols in syntrophic association with methanogenic archaea and are thus called syntrophic bacteria (or syntrophs). Despite plenty of genetic and genomic information being available for primary fermenting bacteria (18, 30) and methanogenic archaea (11, 13, 41), such information is currently scarce for syntrophic bacteria.

A significant feature of syntrophic bacteria is their growth at the thermodynamic limit. For instance, the Gibbs free energy (ΔG°) change in syntrophic propionate oxidation is approximately -25 kJ mol^{-1}, which is less than the energy needed for synthesizing one ATP molecule (44). Syntrophs and methanogens share this energy for their growth. More surprisingly, Jackson and McInerney (22) have shown that substrate oxidation by syntrophs proceeds at values close to the thermodynamic equilibrium ($\Delta G^\circ \approx 0$ kJ mol^{-1}). Therefore, one can deduce that these bacteria should have extremely efficient catabolic systems (22), and their catabolic pathway is of wide biological interest.

Propionate-oxidizing syntrophs have been isolated from mesophilic (4, 16, 27, 47) and thermophilic (21, 34) methanogenic ecosystems. Two propionate-oxidizing pathways have been proposed for mesophilic syntrophic bacteria, i.e., the methylmalonyl-coenzyme A (CoA) pathway (see Fig. 1) and a pathway via a six-carbon intermediate metabolite. The methylmalonyl-CoA (MMC) pathway has first been proposed for methanogenic freshwater sediment (38) and later confirmed for syntrophic propionate-oxidizing bacteria on the basis of the results of ^{13}C-nuclear magnetic resonance analyses of intermediate metabolites (33) and enzyme activity measurements (19). The second pathway has been proposed for *Smithella propionica* (9), which produces acetate and butyrate via a six-carbon intermediate metabolite. In addition, a recent study has detected activities of several enzymes in the MMC pathway in a thermophilic syntrophic propionate-oxidizing bacterium (34). However, there has been no information regarding the genetics of syntrophic propionate oxidation.

The present study was conducted to gain the genetic basis for the central catabolic pathway in a thermophilic syntrophic propionate-oxidizing bacterium, *Pelotomaculum thermopropionicum* strain SI (20, 21). Recent advances in genomics cou-

* Corresponding author. Mailing address: Laboratory of Applied Microbiology, Marine Biotechnology Institute, Heita, Kamaishi, Iwate 026-0001, Japan. Phone: 81-193-26-5781. Fax: 81-193-26-6592. E-mail: kazuya.watanabe@mbio.jp.

pled to database-associated bioinformatics have allowed scientists to identify microbial metabolic pathways on the basis of genome sequences (18, 26, 40). Accordingly, we performed genomic and proteomic analyses of *P. thermopropionicum*, which revealed novel insights into how this organism controls the central metabolic flow and energy production.

MATERIALS AND METHODS

Strains and growth conditions. *P. thermopropionicum* strain SI (DSM 13744) was grown in cultures alone and in cocultures with *Methanothermobacter thermautotrophicus* ΔH (DSM 1053) using a culture medium described elsewhere (21). The medium was supplemented with 0.1% Bacto yeast extract (Difco) and an appropriate fermentation substrate at 20 mM. Cultivation was conducted at 55°C under an atmosphere of N_2 plus CO_2 (80/20 [vol/vol]) without shaking.

DNA isolation and genome-size analysis. *P. thermopropionicum* was grown alone in 1 liter of medium supplemented with fumarate as the sole substrate. Cells were harvested at the late exponential growth phase by centrifugation, and the total DNA was extracted by the method of Marmur (29). To check for the presence of plasmids, the purified DNA was electrophoresed in agarose gels by the standard procedure (37). To determine the genome size, pulsed-field gel electrophoresis was conducted using a contour-clamped homogeneous electric field (CHEF DRIII; Bio-Rad Laboratories) according to the manufacturer's instructions.

Library construction, shotgun sequencing, and assembly. The procedures for draft genome sequencing, namely, shotgun and fosmid library construction, sequencing, and contig assembly, were conducted by Dragon Genomics. Two types of shotgun library were constructed, i.e., a plasmid library containing 2- to 3-kb inserts and a fosmid library containing 30- to 50-kb inserts. For constructing a plasmid library, the extracted DNA was mechanically sheared, blunted, and ligated into HincII-digested pUC118 (Takara). For constructing a fosmid library, the extracted DNA was fractured by the phenol-chloroform treatment, fragments of approximately 33 to 48 kb were recovered by electrophoresis, and they were ligated into pCC1FOS (Epicenter) using a copy control fosmid library production kit (Epicenter). Clones were selected from the plasmid (15,360 clones) and fosmid (960 clones) libraries and subjected to sequencing from both ends by using a DYEnamic ET dye terminator kit (Amersham Bioscience) and a MegaBASE 4000 sequencer (Amersham Bioscience). Raw sequencing data (quality values in the Phred analysis [CodonCode] of more than 15) were assembled to generate "contigs" by using the Paracel genome assembler with the CAP4 algorithm (Paracel). Physically linked contigs were tentatively connected to generate "scaffolds." A scaffold was named CWW_CXX, where CWW and CXX were identification (ID) numbers of the first and last contigs. Gaps were closed where needed by direct sequencing of an PCR-recovered intercontig fragment.

Gene prediction and annotation. The assembled sequences were first analyzed by the GRIMMER 2.10 program (10) trained with the genome sequence of *Clostridium acetobutylicum* ATCC 824 (30). Open reading frames (ORFs) detected were subjected to the BLAST search (49) against the Swiss-Prot (3) and COG (Clusters of Orthologous Groups of proteins) (42) databases to select the ORFs that satisfy the following criteria: sizes larger than 50 amino acids, E values to best-match sequences smaller than 1e−100, best-match sequences being not hypothetical or putative proteins, and the initial and last amino acids being identical to those of the best-match proteins. The GRIMMER program was next trained using the obtained ORFs and again used for analyzing the assembled sequences. After this procedure was repeated three times in total, selected ORFs were subjected to homology search against the COG database using the BLASTp program (1) and the nonredundant GenBank database using the BLASTx program (1). Results of the homology search were linked to the scaffold information and stored in Annotation Viewer (Dragon Genomics) and FileMaker pro version 3.0 (Claris). We also constructed an *P. thermopropionicum* ORF database available for the BLASTp search. The naming scheme for an ORF was CWW_CXX_YY_ZZ (ORF ID number), where CWW_CXX was the ID number of a scaffold, while YY and ZZ were the base numbers of the first and last nucleotides of the ORF.

Functions of ORFs were also analyzed by using the InterPro program (2) linked to the PROSITE, PRINTS, Pfam, SMART, TIGRFAMs, PIR SuperFamily, and ProDom databases to search for conserved domains and motifs and to validate prediction of gene function. The secondary structure and membrane topology were analyzed using the nnPredict (25) and TMpred (17) programs, respectively. Transcription regulation sequences were primarily analyzed using the DBTBS database constructed for analyzing the *Bacillus subtilis* genome (28), and the results were manually checked. Terminator sequences were analyzed using the FindTerm program (SoftBerry). Molecular weights and isoelectric points (pI) of proteins were predicted using the Compute pI/Mw tool (14). Alignment of amino acid sequences was conducted by using the ClustalX program (45) for visually inspecting conservation of motifs and functionally important amino acids. For phylogenetic analyses, a neighbor-joining tree (36) was constructed by using the njplot software in the ClustalX program and plotted by using TREEVIEW (32).

Proteomics. *P. thermopropionicum* cells were grown in cocultures (500 ml) with *M. thermautotrophicus* as described above, harvested by centrifugation at 11,000 × *g* and 4°C for 10 min, and washed two times using 5 mM sodium phosphate buffer (pH 7.0). Each cell pellet was suspended in 25 ml of an Percoll solution (Amersham Bioscience) supplemented with 0.15 M NaCl and subjected to centrifugation at 10,000 × *g* and 4°C for 30 min. After the centrifugation, two distinct bands were seen; microscopic observation showed that the upper band was mostly comprised of cells of *P. thermopropionicum*. We carefully collected this fraction using a pipette, and Percoll particles were removed by washing with the phosphate buffer. The harvested cells were disrupted by sonication (Sonifier 250; Branson), treated with an RNase-DNase solution (1 mg ml^{-1} DNase I, 0.25 mg ml^{-1} RNase A, 0.5 M Tris-HCl [pH 7.0], and 50 mM $MgCl_2$), and lysed in a lysis solution {5 M urea, 2 M thiourea, 4% 3-[(3-cholamidopropyl)dimethylammonio]-1-propane-sulfonate, 80 mM dithiothreitol, and 4% IPG buffer (Amersham Bioscience)}. The resultant lysate was centrifuged at 30,000 × *g* and 4°C for 20 min, and the supernatant was collected. The protein concentration in this supernatant solution was determined using a two-dimensional (2D) Quant kit (Amersham Bioscience).

Two-dimensional gel electrophoresis (2D-GE) was performed using an investigator 2D electrophoresis system (Genomic Solution). Immobiline DryStrip pH 4 to 7 (Amersham Bioscience) was used for the first-dimensional isoelectric focusing, to which approximately 50 μg of protein was loaded. The second-dimensional separation was performed in 12.5% polyacrylamide gels (PAGs) containing 0.1% sodium dodecyl sulfate (SDS). SDS-PAG electrophoresis molecular weight standard low range (Bio-Rad) was used as a size marker. The gels were stained using Sypro Ruby (Molecular Probes) and visualized using the FM BIOII Multi-view system (Hitachi). We performed 2D-GE more than three times for each culture condition and confirmed the reproducibility. Protein spots were quantified using an PDQuest system (Bio-Rad).

For the N-terminal sequencing (NTS) identification, protein spots on an SDS-PAG were transferred to a ProBlott membrane (Applied Biosystems) using an electro membrane blotter (Nippon Eido). Spots were excised from the membrane, and an N-terminal sequence was determined using a 494cLC protein sequencer (Applied Biosystems). For the peptide mass fingerprinting (PMF) identification, a gel was stained using a silver stain kit (Wako). Protein spots were excised and subjected to in-gel trypsin digestion by the method of Katayama et al. (24). Time-of-flight mass spectrometry was performed using a Voyager DE-PRO time-flight mass spectrometer (Applied Biosystems) and α-cyano-4-hydroxycinnamic acid (Sigma) as a matrix. Peptide mass peaks were calibrated using the Data Explorer DM software (Applied Biosystems). Mascot search (Matrix Science) was performed using the *P. thermopropionicum* draft sequence database for identifying protein spots.

Nucleotide sequence accession numbers. The draft genome sequence of *P. thermopropionicum* has been deposited in the DDBJ, EMBL, and NCBI databases under accession numbers BAAC01000001 to BAAC01000195. The accession numbers for nucleotide sequences of Pct3, MmcD, and OdcAB are AB221127, AB221128, and AB221129, respectively.

RESULTS

Draft genome sequencing. Pulsed-field gel electrophoresis determined the genome size of *P. thermopropionicum* to be approximately 3 Mb (data not shown). The genome was single and circular, and no plasmid was found. We performed shotgun sequencing of its genome after constructing plasmid (approximately 2-kb inserts) and fosmid (approximately 42-kb inserts) libraries. A total of 28,453 reads (approximately 17 Mb in total, ×5.5 coverage) generated 105 scaffolds and an assembled sequence of 2,810,264 bp, which was estimated to cover up to 94% of the total genome. Its G+C content was in good agreement with an estimate in a hybridization test (52.8% (21)). In the draft sequence, we found 2,988 of ORFs, of which approximately 70% could be grouped into the COG (42) cat-

TABLE 1. Identification of ORFs relevant to the methylmalonyl-CoA pathway in *P. thermopropionicum*

Putative protein	ORF ID no.	Size (aa)[a]	Homologous protein (function experimentally identified)					Function[b] (step)
			Accession no.	Function	Size (aa)	Host organism	Identity (%)	
Pct1	C269_C272_7114_5546	522	CAB77207	Propionate CoA transferase	524	*Clostridium propionicum*	43	
Pct2	C38_C46_103363_104982	539	CAB77207	Propionate CoA transferase	524	*C. propionicum*	48	
Pct3	C125_C134_3049_1517	525	CAB77207	Propionate CoA transferase	524	*C. propionicum*	56	PCT (I, X)
Tps	C174_C181_70087_68738	450	AAB91834	Y4rI, transposase	390	*Rhizobium* sp. strain NGR234	25	
MmcA	C174_C181_68606_66903	568	P38022	RocR, positive regulator of arginine operon	461	*Bacillus subtilis*	37	
MmcH	C174_C181_60782_59241	513	CAA80872	Methylmalonyl-CoA decarboxylase, alpha subunit	509	*Veillonella parvula*	61	
			AAA25676	Transcarboxylase, 12S subunit	610	*Propionibacterium freudenreichii*	57	
MmcI	C174_C181_59207_59010	65	CAA80874	Methylmalonyl-CoA decarboxylase, epsilon subunit	55	*V. parvula*	36	POT (II, VIII)
MmcJ	C174_C181_58962_58522	146	CAA80875	Methylmalonyl-CoA decarboxylase, gamma subunit	129	*V. parvula*	58	
			AAA25674	Transcarboxylase, 1.3S subunit	123	*P. freudenreichii*	41	
MmcL	C174_C181_57456_56056	466	AAA03174	Transcarboxylase, 5S subunit	505	*P. freudenreichii*	47	
MmcG	C174_C181_61199_60798	133	AAK52053	Methylmalonyl-CoA epimerase	132	*Pyrococcus horikoshii*	65	MCE
MmcE	C174_C181_63424_61751	557	CAA33090	Methylmalonyl-CoA mutase, α subunit, N-terminal	782	*P. freudenreichii*	51	MCM (III)
MmcF	C174_C181_61734_61333	133	CAA33090	Methylmalonyl-CoA mutase, α subunit, C-terminal	782	*P. freudenreichii*	43	
MmcD1	C174_C181_64720_63857	369	AAA23899	Succinyl-CoA synthetase, beta subunit	388	*Escherichia coli*	42	SCS (IV)
MmcD2	C174_C181_63856_63455	290	AAA23900	Succinyl-CoA synthetase, alpha subunit	289	*E. coli*	53	
Sdh1A	C299_C301_4906_5607	233	P17413	Succinate dehydrogenase, cytochrome *b* subunit	256	*Wolinella succinogenes*	25	
Sdh1B	C299_C301_5607_7433	608	P17412	Succinate dehydrogenase, flavoprotein subunit	656	*W. succinogenes*	59	SDH (V)
Sdh1C	C299_C301_7463_8212	249	P17596	Succinate dehydrogenase, iron-sulfur subunit	239	*W. succinogenes*	55	
Sdh2A	C488_C492_41583_40369	404	AAB84847	F420-reducing hydrogenase, beta subunit	406	*M. thermautotrophicus*	29	
Sdh2B	C488_C492_40372_38630	582	P17412	Succinate dehydrogenase, flavoprotein subunit	656	*W. succinogenes*	39	SDH (V)
Sdh2C	C488_C492_38626_37982	212	P17596	Succinate dehydrogenase, iron-sulfur subunit	239	*W. succinogenes*	33	
MmcB	C174_C181_66625_65783	280	AAA72317	Fumarase, N-terminal domain	514	*Bacillus stearothermophilus*	34	FHT (VI)
MmcC	C174_C181_65736_65173	187	AAA72317	Fumarase, C-terminal domain	514	*B. stearothermophilus*	38	
MmcK	C174_C181_58432_57494	312	CAA62129	Malate dehydrogenase	312	*Bacillus israeli*	62	MDH (VII)
OdcA	C107_C113_14778_12932	637	AAG45426	Pyruvate carboxylase, biotin-containing subunit	573	*Methanosarcina barkeri*	48	ODC (VIII)
OdcB	C107_C113_12921_11539	455	AAG45427	Pyruvate carboxylase, ATP-binding subunit	493	*M. barkeri*	58	
MmcM	C174_C181_55929_52411	1,172	CAC2229	Pyruvate:ferredoxin oxidoreductase	1,171	*C. acetobutylicum*	66	POR (IX)
Pfl1	C424_C425_11671_9164	835	CAA30828	Pyruvate formate lyase	810	*E. coli*	30	PFL (IX)
Acs1	C197_C201_61557_59689	622	YP_219141	Short-chain acyl-coenzyme A synthetase	652	*Salmonella enterica*	58	ACS (X)
Adh1	C416_C423_11766_10603	387	A25978	Alcohol dehydrogenase, ethanol transforming	383	*Zymomonas mobilis*	56	ADH
Adh2	C360_C366_4915_3764	383	A25978	Alcohol dehydrogenase, ethanol transforming	383	*Z. mobilis*	40	ADH
Adh3	C475_C479_1134_16	372	A25978	Alcohol dehydrogenase, ethanol transforming	383	*Z. mobilis*	41	ADH
Adh4, partial	C33_C37_11275_10610	222	A25978	Alcohol dehydrogenase, ethanol transforming	383	*Z. mobilis*	41	ADH
Aor1	C202_C206_43009_44802	597	CAA56170	Aldehyde:ferredoxin oxidoreductase	605	*Pyrococcus furiosus*	47	AOR
Aor2, partial	C33_C37_13241_11820	474	CAA56170	Aldehyde:ferredoxin oxidoreductase	605	*P. furiosus*	36	AOR
Aor3	C416_C423_6968_4983	661	CAA56170	Aldehyde:ferredoxin oxidoreductase	605	*P. furiosus*	46	AOR
Aor4	C466_C471_9292_11172	626	CAA56170	Aldehyde:ferredoxin oxidoreductase	605	*P. furiosus*	43	AOR
Aor5	C466_C471_18800_20632	610	CAA56170	Aldehyde:ferredoxin oxidoreductase	605	*P. furiosus*	38	AOR
Aor6	C466_C471_36968_38818	616	CAA56170	Aldehyde:ferredoxin oxidoreductase	605	*P. furiosus*	37	AOR
Aor7	C480_C487_5561_7285	574	CAA56170	Aldehyde:ferredoxin oxidoreductase	605	*P. furiosus*	36	AOR
Aad1	C38_C46_93919_96621	900	AAA81906	Alcohol dehydrogenase 2	870	*Entamoeba histolytica*	52	AAD
KorA	C475_C479_4138_5277	379	O27112	2-Oxoglutarate:ferredoxin oxidoreductase, alpha subunit	378	*M. thermautotrophicus*	52	
KorB	C475_C479_5291_6127	275	O27113	2-Oxoglutarate:ferredoxin oxidoreductase, beta subunit	286	*M. thermautotrophicus*	52	KOR
KorC	C475_C479_6135_6710	191	O27114	2-Oxoglutarate:ferredoxin oxidoreductase, gamma subunit	189	*M. thermautotrophicus*	44	

Ldh1	C442_C447_5883_4945	310	AAP34686	Lactate dehydrogenase	292	Thermoanaerobacterium saccharolyticum	51	LDH
Pps1	C448_C454_22708_25392	894	Q59754	Pyruvate orthophosphate dikinase	898	*Sinorhizobium meliloti*	56	PPS
Hyd1	C174_C181_43188_44984	599	P29166	Fe-only hydrogenase	574	*Clostridium pasteurianum*	40	
Hyd2	C495_C500_60438_58795	548	P29166	Fe-only hydrogenase	574	*C. pasteurianum*	35	
Hyd3, partial	C2_C3_13864_15483	540	P29166	Fe-only hydrogenase	574	*C. pasteurianum*	41	
Hyd4A	C38_C46_19959_18922	346	P13063	Periplasmic [NiFeSe] hydrogenase, small subunit	315	*Desulfomicrobium baculatum*	40	
Hyd4B	C38_C46_18899_17454	482	P13065	Periplasmic [NiFeSe] hydrogenase, large subunit	514	*D. baculatum*	49	
Fdx1	C152_C156_19892_19677	72	Q57610	Ferredoxin	69	*Methanocaldococcus jannaschii*	39	
Fdx2	C22_C23_13454_13741	96	P00202	Ferredoxin		*Methanosarcina barkeri*	38	
Fdx3	C350_C353_13822_14151	110	P00202	Ferredoxin	59	*M. barkeri*	42	
Fdx4	C416_C423_19509_19237	91	P68646	Ferredoxin-like protein	98	*E. coli*	37	
Fdx5	C448_C454_31020_31199	60	P00211	Ferredoxin II	56	*Desulfovibrio desulfuricans*	44	
Fdx6	C488_C492_6291_6052	80	P00203	Ferredoxin	63	*Moorella thermoacetica*	48	
AtpA	C19_C21_9659_10405	249	P37813	ATP synthase, A chain	244	*B. subtilis*	36	
AtpB	C19_C21_10506_10739	78	P37815	ATP synthase, C chain	70	*B. subtilis*	61	
AtpC	C19_C21_10931_11434	168	P37814	ATP synthase, B chain	170	*B. subtilis*	36	
AtpD	C19_C21_11431_11991	187	P37811	ATP synthase, delta chain	181	*B. subtilis*	35	
AtpE	C19_C21_12017_13534	506	P37808	ATP synthase, alpha chain	502	*B. subtilis*	62	
AtpF	C19_C21_13678_14529	284	P37810	ATP synthase, gamma chain	290	*B. subtilis*	49	
AtpG	C19_C21_14561_15970	470	P37809	ATP synthase, beta chain	473	*B. subtilis*	70	
AtpH	C19_C21_15993_16394	134	P37812	ATP synthase, gamma chain	132	*B. subtilis*	50	

[a] aa, amino acids.
[b] Abbreviations were as follows (except for those appearing in the legend to Fig. 1): MCE, methylmalonyl-CoA epimerase; ODC, oxaloacetate decarboxylase; POR, pyruvate:ferredoxin oxidoreductase; PFL, pyruvate formate lyase; ACS, acetyl-CoA synthetase; ADH, alcohol dehydrogenase; AOR, aldehyde:ferredoxin oxidoreductase; AAD, alcohol/aldehyde dehydrogenase; KOR, 2-oxoglutarate:ferredoxin oxidoreductase; LDH, lactate dehydrogenase; PPS, phosphoenolpyruvate synthetase. Refer to Fig. 2 for enzyme reactions.

FIG. 1. Proposed methylmalonyl-CoA pathway (modified from reference 37). PCT, propionate CoA transferase; POT, propionyl-CoA: oxaloacetate transcarboxylase; MCM, methylmalonyl-CoA mutase; SCS, succinyl-CoA synthetase; SDH, succinate dehydrogenase; FHT, fumarate hydratase (fumarase); MDH, malate dehydrogenase; PDH, pyruvate dehydrogenase.

egories (data not shown). On the basis of the current draft data, we constructed ORF databases available for keyword and BLAST searches (these databases will be provided on request).

Reconstruction of the central catabolic pathway. *P. thermopropionicum* is capable of anaerobic growth on propionate, propanol, butanol, ethanol, and lactate in cocultures with a hydrogenotrophic methanogen, such as *Methanothermobacter thermautotrophicus* ΔH, while it can also grow on fumarate and pyruvate in culture alone (21). It is known that this bacterium produces acetate and propionate (at a molar ratio of 3:1) from pyruvate (21). Since the available substrates and fermentation products are either constituents of the MMC pathway or compounds directly linked to this pathway, we assumed that *P. thermopropionicum* likely utilized the MMC pathway (Fig. 1) for metabolizing propionate.

No genetic information had been available for the MMC pathway. However, since genes for enzymes functionally identical to those in this pathway have been identified in other organisms, such as genes for enzymes in the citrate cycle in aerobic bacteria and those in the propionate fermentation pathway in *Propionibacterium acnes* (5), we were able to search for putative genes for enzymes in the MMC pathway. We picked ORFs of interest by keyword and BLAST search against the *P. thermopropionicum* ORF databases, for which we selected search terms and sequences according to information obtained from the KEGG (Kyoto Encyclopedia of Genes and Genomes) pathway database (23). The selected ORFs were further analyzed for the conservation of signature motifs and important amino acids and, in some cases, similarities in the overall structures. ORFs in the draft genome sequence for Pct3, MmcD, and OdcA (Table 1) were found over two contigs, whose sequences were later completed and independently deposited to the databases (information available from authors upon request).

Table 1 summarizes results of the ORF search, showing that ORFs for all enzymes in the MMC pathway (Fig. 1) were identified. Of the enzymes in the MMC pathway that are dif-

ferent from previously known enzymes, methylmalonyl-CoA mutase (MCM) and fumarate hydratase (FHT) (fumarase) seem to be composed of two different subunits (information available from authors upon request). The two-subunit FHT enzyme was expressed in *Escherichia coli*, and its fumarate-transforming activity was detected at 55°C (our unpublished result). We also found an ORF for methylmalonyl-CoA epimerase (MCE) [which catalyzes isomerization between (*R*)-methylmalonyl-CoA and (*S*)-methylmalonyl-CoA], which should be necessary prior to step III (Fig. 1). Pyruvate:ferredoxin oxidoreductase (POR), rather than pyruvate dehydrogenase (PDH), was found in the *P. thermopropionicum* genome (Table 1), which is known to utilize low-potential ferredoxin as an electron acceptor. It was also found that each of the last three steps in this pathway, oxaloacetate decarboxylation (step VIII), acetyl-CoA formation (step IX), and acetyl-CoA hydrolysis (step X), can be catalyzed by two different enzymes (Table 1). According to the genomic information, we reconstructed the MMC pathway in *P. thermopropionicum* (Fig. 2).

An interesting feature found in the sequence analysis was that many ORFs for the enzymes in the MMC pathway, except for those for propionate CoA transferase (PCT) and SDH, formed a tight cluster on the genome (*mmcBCDEFGHIJKLM* in Fig. 3), which we named the *mmc* cluster. We also found two ORFs (*tps* and *mmcA*) upstream of this cluster (Table 1 and Fig. 3). MmcA is homologous (37% identical in total amino acids) to RocR, an NtrC/NifA family transcriptional regulator in *B. subtilis* (7). Analyses of two long intergenic regions (*mmcA-mmcB* [274 bp] and *mmcC-mmcD* [452 bp]) performed using the DBTBS database (28) found that there existed a consensus sequence for a sigma L-dependent promoter (8) in the *mmcA-mmcB* intergenic region, while consensus sequences for sigma H-dependent promoters (12) and sigma A-dependent promoters (48) were present in the *mmcC-mmcD* region (data not shown).

Peripheral pathways. We also found ORFs that showed substantial homologies to genes for enzymes catalyzing peripheral pathways of the MMC pathways (Table 1 and Fig. 2), such as lactate dehydrogenase (LDH), 2-oxoglutarate:ferredoxin oxidoreductase (KOR), and phosphoenolpyruvate synthetase (PPS). LDH is considered to be used for growth of this bacterium on lactate, while KOR and PPS are important for linking the MMC pathway to biosyntheses of cellular components.

P. thermopropionicum is capable of growth on several short-chain alcohols, such as ethanol, propanol, and butanol. The end product from butanol is butyrate, while propionate produced from propanol is further transformed to acetate. Our growth test showed that acetate and propionate were produced from ethanol (data not shown). In the genome of *P. thermopropionicum*, multiple ORFs for alcohol dehydrogenase (ADH) and aldehyde:ferredoxin oxidoreductase (AOR) and one ORF for alcohol/aldehyde dehydrogenase (AAD) were identified (Table 1 and Fig. 2). A combination of ADH and AOR produces acetate from ethanol, while AAD directly produces acetyl-CoA. Substrates for these ADHs and AORs need to be experimentally identified.

We found ORFs for four hydrogenases (three Fe-only hydrogenases and one NiFeSe hydrogenase [Table 1]) in the draft genome; these ORFs may be important for scavenging reducing equivalents produced in the MMC pathway and alcohol metabolism as molecular hydrogen. As electron carriers, six ORFs for ferredoxins were found (Table 1), while there was no ORF for a soluble *c*-type cytochrome. A complete set of ORFs for bacterial F-type ATPase was also identified (Table 1).

Proteomic analyses. In order to detect proteins encoded by ORFs in the *mmc* cluster, we carried out 2D-GE proteomic analysis of soluble proteins in cells grown on propionate or butanol (Fig. 4). In this analysis, the amounts of proteins loaded on a gel were optimized for evaluating the levels of expression of major soluble proteins. The butanol culture was chosen as the control, because its catabolism is not linked to the MMC pathway. We used the draft genome data to identify major protein spots by PMF and/or NTS. As summarized in Table 2, we were able to detect subunits of propionyl-CoA:oxaloacetase transcarboxylase (POT) (McmH), MCM (MmcE), succinyl-CoA synthetase (SCS) (MmcD1), malate dehydrogenase (MDH) (MmcK), FHT (MmcB), and succinate dehydrogenase (SDH) (Sdh1C) as major spots in the gel. MCE and POR were undetected, probably because their sizes were out of the range of the gel. However, we assume that they were also expressed, since the genes of these enzymes were present in the same transcriptional unit (Fig. 3). In addition, we could not detect the predicted PCT (Pct3 in Table 1), whereas a subunit of an alternative putative CoA transferase (spot 17) was detected. This transferase is homologous (31% identical in amino acids) to GctA, a subunit of glutaconate CoA-transferase from *Acidaminococcus fermentans* (CAA57199). Although spot 17 was not specifically expressed in the propionate culture, we also need to consider a possibility that this protein functions as PCT.

We next determined the relative intensity of each protein spot (the intensity of a spot was divided by the sum of intensities of all spots in a gel) and compared them between the propionate and butanol cultures (Table 2). MmcK and MmcB each appeared as two spots (spots 15 and 16 and spots 18 and 19, respectively), whose average ratios in the relative intensity were 2.3 and 4.8, respectively. This analysis showed that the enzymes in the MMC pathway were generally up-regulated in the propionate culture and that the up-regulation of MmcB was the most stringent. These tendencies of changes in the spot intensity were also observed when the propionate culture was compared with the propanol or ethanol culture (data not shown).

DISCUSSION

In the present study, we carried out draft sequencing of the genome of *P. thermopropionicum* to obtain the genetic basis for its central metabolic pathway. In combination with the results of the proteomic analysis, we conclude that this thermophilic syntroph utilizes the MMC pathway for propionate oxidation. The draft sequencing and subsequent targeted gap closing provided the complete sequences for genes encoding the enzymes necessary for reconstructing the MMC pathway, which will assist in subsequent studies for biochemical characterization of the enzymes and molecular analyses of transcriptional regulation mechanisms. Below, we discuss some aspects of the central catabolic pathway in *P. thermopropionicum* on the basis of current genomic information.

A similar pathway has been identified as a propionate-fermenting pathway in the genome of *Propionibacterium acnes*

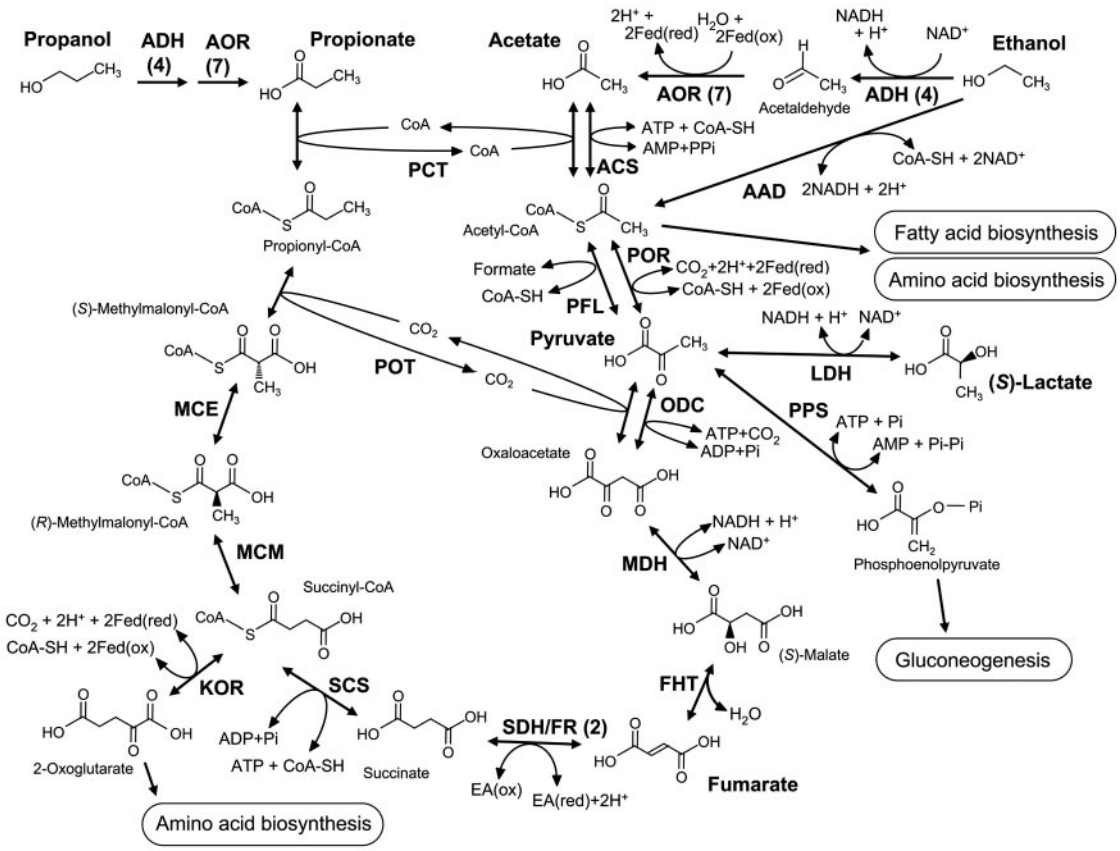

FIG. 2. Reconstructed MMC pathway in *P. thermopropionicum* based on the genomic data. See the explanations for abbreviations in the legend for Fig. 1 and footnote *b* of Table 1. When there is more than one ORF, the numbers of ORFs found in the genome are presented in parentheses. Fed(red) and Fed(ox), reduced and oxidized ferredoxin, respectively; FR, fumarate reductase; EA, electron acceptor.

(5), while we found differences between the MMC pathway in *P. thermopropionicum* and the propionate-fermenting pathway in *P. acnes*. First, *P. acnes* utilizes a malic enzyme catalyzing the conversion between malate and pyruvate (malate + NAD^+ = pyruvate + CO_2 + NADH) for steps VII and VIII. Second, PCT is used for step I in *P. thermopropionicum*, while the same reaction is catalyzed by propionyl-CoA synthetase in *P. acnes*.

The first two steps in the MMC pathways in *P. thermopropionicum* (steps I and II in Fig. 1) are catalyzed by transferases, i.e., PCT and POT. These enzymes require counterpart substrates for their activities (CoA derivatives, e.g., acetyl-CoA, for PCT and oxaloacetate for POT), while these counterparts are also the downstream intermediate metabolites in the MMC pathway. We think that this is one of the reasons why growth of *P. thermopropionicum* was so slow. As reported previously (20), growth of this bacterium on propionate in coculture with a hydrogenotrophic methanogen occurred after a long lag period of ~20 days. It is likely that this lag period is necessary for *P. thermopropionicum* to accumulate these counterpart substrates, and propionate oxidation is initiated only after the concentrations of these substrates reach certain levels. Another possibility for the long lag period would be that the cells need much time for the expression of the catabolic enzymes under the energy-limiting conditions.

Proteomic analyses (Fig. 4 and Table 2) showed that a subunit of fumarase (MmcB) was up-regulated in the propionate culture compared to the butanol culture. Other proteins identified to be encoded in the *mmc* cluster were also up-regulated in the propionate culture, although up-regulation of these proteins was weaker than that of MmcB. Northern blot analysis confirmed this tendency of gene expression regulation (our unpublished results). We think that this tendency reflected the genetic organization of the *mmc* cluster. As shown in Fig. 3, the sequence analysis suggested that transcription of *mmcBC* is

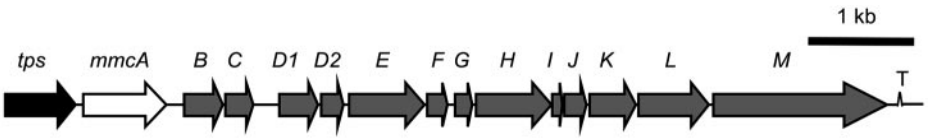

FIG. 3. Genetic organization of the *mmc* cluster. For ORF names, refer to Table 1. The transposase gene (black arrow), regulatory gene (white arrow), and *mmc* structural genes (gray arrows) are indicated. T, terminator.

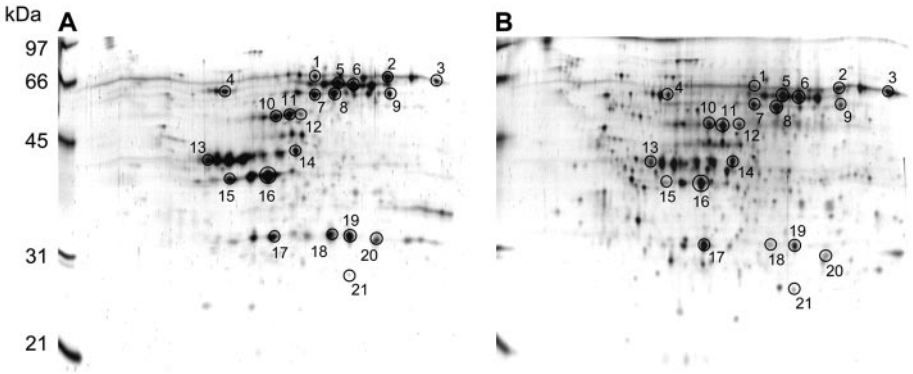

FIG. 4. 2D-GE patterns of soluble proteins in *P. thermopropionicum* cells recovered from coculture with *M. thermautotrophicus*. The growth substrates were propionate (A) and butanol (B). The circled protein spots were excised and identified (Table 2).

solely regulated by the sigma L-dependent promoter, while that of *mmcDEFGHIJKLM* is also under the control of the sigma A and H-dependent promoters. Sigma A is known to be the major sigma factor in *B. subtilis* (48), which corresponds to sigma 70 in gram-negative bacteria (15). Sigma A has been considered to control expression of approximately 250 operons in *B. subtilis*, many of which encode housekeeping proteins (the DBTBS database). Sigma H is a nonessential sigma factor involved in the expression of vegetative and early stationary-phase genes in *B. subtilis* (12). We found 19 ORFs for sigma factors in the draft genome of *P. thermopropionicum*; these ORFs include 1 ORF for sigma A, 2 ORFs for sigma H, and 1ORF for sigma L (data not shown). These findings suggest that *mmcDEFGHIJKLM* are transcribed at certain levels under a wide range of growth conditions. In contrast, sigma L is a member of the sigma 54 family of bacterial sigma factors, which are characterized by their cooperative action with enhancer-binding proteins whose function requires nucleotide

TABLE 2. Characterization of major protein spots on the 2D gels

Spot	Identification[a]	ORF ID number	Function	Predicted value		Relative intensity[b]		Ratio[c]
				pI	MW	Propionate	Butanol	
1	PMF (92)	C174_C181_63424_61751	MmcE, methylmalonyl-CoA mutase, N-terminal domain	5.3	58,372	0.0129 ± 0.0023	0.0048 ± 0.0003	2.7
2	PMF (111)	C2_C3_12091_13788	NADH:ubiquinone oxidoreductase, NADH-binding subunit	6.2	59,639	0.0283 ± 0.0014	0.0235 ± 0.0032	1.2
3	PMF (125)	C2_C3_12091_13788	NADH:ubiquinone oxidoreductase, NADH-binding subunit	6.2	59,639	0.0197 ± 0.0043	0.0269 ± 0.0054	0.7
4	PMF (92)	C480_C487_3441_5072	GroEL, 60-kDa chaperonin	4.9	52,334	0.0102 ± 0.0009	0.0138 ± 0.0015	0.7
5	NTS (11)	C2_C3_13867_15483	Hydrogenase (partial)	ND[d]	ND	0.0291 ± 0.0028	0.0231 ± 0.0013	1.3
6	NTS (7)	C2_C3_13867_15483	Hydrogenase (partial)	ND	ND	0.0292 ± 0.0051	0.0321 ± 0.0050	0.9
7	PMF (193)	C19_C21_12017_13534	F_oF_1-type ATP synthase, alpha subunit	5.7	55,200	0.0185 ± 0.0009	0.0207 ± 0.0028	0.9
8	NTS (8)	C19_C21_12017_13534	F_oF_1-type ATP synthase, alpha subunit	5.7	55,200	0.0160 ± 0.0005	0.0141 ± 0.0012	1.1
9	PMF (110)	C174_C181_60782_59241	MmcH, transcarboxylase, 12S subunit	6.0	56,039	0.0063 ± 0.0001	0.0042 ± 0.0001	1.5
10	PMF (219)	C19_C21_14561_15970	F_oF_1-type ATP synthase, beta subunit	5.4	50,858	0.0209 ± 0.0020	0.0139 ± 0.0022	1.5
11	PMF (265)	C19_C21_14561_15970	F_oF_1-type ATP synthase, beta subunit	5.4	50,858	0.0242 ± 0.0013	0.0266 ± 0.0025	0.9
12	PMF (71)	C19_C21_14561_15970	F_oF_1-type ATP synthase, beta subunit	5.4	50,858	0.0090 ± 0.0011	0.0067 ± 0.0009	1.4
13	NTS (12)	C174_C181_64720_63857	MmcD1, succinyl-CoA synthase	5.1	44,748	0.0300 ± 0.0050	0.0125 ± 0.0043	2.4
14	PMF (61)/NTS (14)	C416_C423_11766_10603	Alcohol dehydrogenase class IV	6.2	45,226	0.0162 ± 0.0005	0.0172 ± 0.0030	0.9
15	PMF (125)	C174_C181_58432_57494	MmcK, malate dehydrogenase	5.3	32,875	0.0215 ± 0.0011	0.0043 ± 0.0004	5.0
16	PMF (170)/NTS (12)	C174_C181_58432_57494	MmcK, malate dehydrogenase	5.3	32,875	0.0416 ± 0.0059	0.0227 ± 0.0015	1.8
17	PMF (113)/NTS (12)	C125_C134_84754_83942	Acyl CoA:acetate/β-ketoacid CoA transferase beta subunit	5.3	29,233	0.0271 ± 0.0022	0.0261 ± 0.0016	1.0
18	PMF (108)/NTS (10)	C174_C181_66625_65783	MmcB, fumarase N-terminal domain	5.8	26,869	0.0206 ± 0.0012	0.0023 ± 0.0008	9.0
19	PMF (103)/NTS (12)	C174_C181_66625_65783	MmcB, fumarase N-terminal domain	5.8	26,869	0.0308 ± 0.0017	0.0085 ± 0.0012	3.6
20	PMF (126)	C299_C301_7463_8212	Sdh1C, succinate dehydrogenase/ fumarate reductase iron sulfur subunit	6.2	28,183	0.0131 ± 0.0008	0.0080 ± 0.0016	1.6
21	PMF (57)	C436_C439_1992_2702	Branched-chain amino acid ABC transporter	5.8	26,020	0.0028 ± 0.0001	0.0034 ± 0.0003	0.8

[a] Methods for identification were PMF (peptide mass fingerprinting), NTS (N-terminal sequencing), or both. For PMF, mascot search scores expressing probabilities of PMF identification are presented in parentheses. The scores greater than 47 are significant ($P < 0.05$). For NTS, the numbers of amino acid residues determined are indicated in parentheses. All amino acid residues determined were matched to predicted residues.

[b] Relative intensity was estimated by dividing the intensity of a spot by the sum of intensities of all spots detected on a gel. Values are means ± standard deviations ($n = 3$).

[c] Ratio of relative intensity for the propionate culture to that for the butanol culture.

[d] ND, not determined.

hydrolysis (6). Many sigma 54-controlled genes are specifically transcribed in the presence of enhancer molecules (6). In the case of the *mmc* cluster, it is likely that MmcA functions as an enhancer-binding protein, although we have not yet identified what molecules (or conditions) actually enhanced the expression of *mmcBC*. Since MmcA includes the PAS domain (43), we deduce that expression of MmcB is enhanced by a global physiological status, e.g., the membrane potential (43), rather than a specific substrate of the catabolic pathway. Up-regulation of the other MMC proteins may also be governed by the sigma L-dependent promoter, although its regulation may be weakened by the other promoters.

As discussed above, the genome analyses suggested that the particular genetic organization of *P. thermopropionicum* has evolved to accomplish the hierarchical transcriptional regulation of its central metabolic pathway. We think that the stringent regulation of fumarase is physiologically expedient in terms of multiple roles of fumarate in that system. First, since fumarate is an intermediate metabolite of the propionate-oxidizing pathway, fumarase should be up-regulated together with other MMC enzymes, when the bacterium metabolizes propionate. In addition, fumarate is a growth substrate in the culture of *P. thermopropionicum* alone, where *P. thermopropionicum* primarily oxidizes it to acetate, while this organism also utilizes it as an electron acceptor to form succinate (namely, fumarate disproportionation [46]) (Fig. 2). As shown in Fig. 4 and Table 2, the expression of fumarase was conditional, while that of fumarate reductase (i.e., Sdh1C, spot 20 in Fig. 4) did not show much change. It is beneficial for *P. thermopropionicum* to mainly utilize fumarate as the electron acceptor when the MMC pathway does not efficiently work, because fumarate respiration can produce the membrane proton gradient. Proteomics (Table 2 and Fig. 4) showed that *P. thermopropionicum* expressed a significant amount of ATPase, suggesting that this organism can utilize reducing equivalents produced by fermentation for fumarate respiration and oxidative phosphorylation. It is worth noting that two putative SDHs are present in this organism (Table 1); their roles will be addressed in future biochemical studies. All together, we suggest that fumarase acts as the central metabolic switch controlling the metabolic flow and energy conservation in this syntrophic bacterium.

In conclusion, the genomic analyses of *P. thermopropionicum* offer a glimpse into the sophisticated catabolic system of syntrophic bacteria. Owing to its unique genetic organization, the *mmc* cluster may also be interesting for scientists who investigate the evolutionary aspects of operon formation (31, 35). We are currently conducting genetic and biochemical experiments for more-quantitative evaluations of the contribution of each promoter under different growth conditions.

ACKNOWLEDGMENTS

We thank Yasuo Igarashi (University of Tokyo) for helpful advice and continuous encouragement. Acknowledgment is also made to Youhei Urushida for N-terminal amino acid sequencing and Reiko Hirano for technical assistance.

This work was supported by New Energy and Industrial Technology Development Organization (NEDO).

REFERENCES

1. **Altschul, S., T. Madden, A. Schaffer, J. Zhang, Z. Zhang, W. Miller, and D. J. Lipman.** 1997. Gapped BLAST and PSI-BLAST: a new generation of protein database search programs. Nucleic Acids Res. **25:**3389–3402.
2. **Apweiler, R., T. K. Attwood, A. Bairoch, A. Bateman, E. Birney, M. Biswas, P. Bucher, L. Cerutti, F. Corpet, M. D. Croning, R. Durbin, L. Falquet, W. Fleischmann, J. Gouzy, H. Hermjakob, N. Hulo, I. Jonassen, D. Kahn, A. Kanapin, Y. Karavidopoulou, R. Lopez, B. Marx, N. J. Mulder, T. M. Oinn, M. Pagni, F. Servant, C. J. Sigrist, and E. M. Zdobnov.** 2001. The InterPro database, an integrated documentation resource for protein families, domains and functional sites. Nucleic Acids Res. **29:**37–40.
3. **Boeckmann, B., A. Bairoch, R. Apweiler, M. Blatter, A. Estreicher, E. Gasteiger, M. Martin, K. Michoud, C. O'Donovan, I. Phan, S. Pilbout, and M. Schneider.** 2003. The SWISS-PROT protein knowledge base and its supplement TrEMBL in 2003. Nucleic Acids Res. **31:**365–370.
4. **Boone, D. R., and M. P. Bryant.** 1980. Propionate-degrading bacterium, *Syntrophobacter wolinii* sp. nov., gen. nov., from methanogenic ecosystems. Appl. Environ. Microbiol. **40:**626–632.
5. **Brüggemann, H., A. Henne, F. Hoster, H. Liesegang, A. Wiezer, A. Strittmatter, S. Hujer, P. Durre, and G. Gottschalk.** 2004. The complete genome sequence of *Propionibacterium acnes*, a commensal of human skin. Science **305:**671–673.
6. **Buck, M., M. T. Gallegos, D. J. Studholme, Y. Guo, and J. D. Gralla.** 2000. The bacterial enhancer-dependent σ^{54} (σ^{N}) transcription factor. J. Bacteriol. **182:**4129–4136.
7. **Calogero, S., R. Gardan, P. Glaser, J. Schweizer, G. Rapoport, and M. Debarbouille.** 1994. RocR, a novel regulatory protein controlling arginine utilization in *Bacillus subtilis*, belongs to the NtrC/NifA family of transcriptional activators. J. Bacteriol. **176:**1234–1241.
8. **Debarbouille, M., I. Martin-Verstraete, F. Kunst, and G. Rapoport.** 1991. The *Bacillus subtilis sigL* gene encodes an equivalent of sigma 54 from Gram-negative bacteria. Proc. Natl. Acad. Sci. USA **88:**9092–9096.
9. **De Bok, F. A., A. J. Stams, C. Dijkema, and D. R. Boone.** 2001. Pathway of propionate oxidation by a syntrophic culture of *Smithella propionica* and *Methanospirillum hungatei*. Appl. Environ. Microbiol. **67:**1800–1804.
10. **Delcher, A. L., D. Harmon, S. Kasif, O. White, and S. L. Salzberg.** 1999. Improved microbial gene identification with GLIMMER. Nucleic Acids Res. **27:**4636–4641.
11. **Deppenmeier, U., A. Johann, T. Hartsch, R. Merkl, R. A. Schmitz, R. Martinez-Arias, A. Henne, A. Wiezer, S. Baumer, C. Jacobi, H. Bruggemann, T. Lienard, A. Christmann, M. Bomeke, S. Steckel, A. Bhattacharyya, A. Lykidis, R. Overbeek, H. P. Klenk, R. P. Gunsalus, H. J. Fritz, and G. Gottschalk.** 2002. The genome of *Methanosarcina mazei*: evidence for lateral gene transfer between Bacteria and Archaea. J. Mol. Microbiol. Biotechnol. **4:**453–461.
12. **Dubnau, E., J. Weir, G. Nair, L. Carter III, C. Moran, Jr., and I. Smith.** 1988. *Bacillus* sporulation gene *spo0H* codes for σ^{30} (σ^{H}). J. Bacteriol. **170:**1054–1062.
13. **Galagan, J. E., C. Nusbaum, A. Roy, M. G. Endrizzi, P. Macdonald, W. FitzHugh, S. Calvo, R. Engels, S. Smirnov, D. Atnoor, A. Brown, N. Allen, J. Naylor, N. Stange-Thomann, K. DeArellano, R. Johnson, L. Linton, P. McEwan, K. McKernan, J. Talamas, A. Tirrell, W. Ye, A. Zimmer, R. D. Barber, I. Cann, D. E. Graham, D. A. Grahame, A. M. Guss, R. Hedderich, C. Ingram-Smith, H. C. Kuettner, J. A. Krzycki, J. A. Leigh, W. Li, J. Liu, B. Mukhopadhyay, J. N. Reeve, K. Smith, T. A. Springer, L. A. Umayam, O. White, R. H. White, E. Conway de Macario, J. G. Ferry, K. F. Jarrell, H. Jing, A. J. Macario, I. Paulsen, M. Pritchett, K. R. Sowers, R. V. Swanson, S. H. Zinder, E. Lander, W. W. Metcalf, and B. Birren.** 2002. The genome of *M. acetivorans* reveals extensive metabolic and physiological diversity. Genome Res. **12:**532–542.
14. **Gasteiger, E., C. Hoogland, A. Gattiker, S. Duvaud, M. R. Wilkins, R. D. Appel, and A. Bairoch.** 2005. Protein identification and analysis tools on the ExPASy server, p. 571–607. *In* J. M. Walker (ed.), The proteomics protocols handbook. Humana Press, Totowa, N.J.
15. **Gitt, M. A., L. F. Wang, and R. H. Doi.** 1985. A strong sequence homology exists between the major RNA polymerase sigma factors of *Bacillus subtilis* and *Escherichia coli*. J. Biol. Chem. **260:**7178–7185.
16. **Harmsen, H. J., B. L. van Kuijk, C. M. Plugge, A. D. Akkermans, W. M. de Vos, and A. J. Stams.** 1998. *Syntrophobacter fumaroxidans* sp. nov., a syntrophic propionate-degrading sulfate-reducing bacterium. Int. J. Syst. Bacteriol. **48:**1383–1387.
17. **Hofmann, K., and W. Stoffel.** 1993. TMPred—a database of membrane spanning protein segments. Biol. Chem. Hoppe-Seyler **347:**166.
18. **Hong, S. H., J. S. Kim, S. Y. Lee, Y. H. In, S. S. Choi, J. K. Rih, C. H. Kim, H. Jeong, C. G. Hur, and J. J. Kim.** 2004. The genome sequence of the capnophilic rumen bacterium *Mannheimia succiniciproducens*. Nat. Biotechnol. **22:**1275–1281.
19. **Houwen, F. P., J. Plokker, A. J. M. Stams, and A. J. B. Zehnder.** 1990. Enzymatic evidence for involvement of the methylmalonyl-CoA pathway in propionate oxidation by *Syntrophobacter wolinii*. Arch. Microbiol. **155:**52–55.
20. **Imachi, H., Y. Sekiguchi, Y. Kamagata, A. Ohashi, and H. Harada.** 2000. Cultivation and in situ detection of a thermophilic bacterium capable of oxidizing propionate in syntrophic association with hydrogenotrophic methanogens in a thermophilic methanogenic granular sludge. Appl. Environ. Microbiol. **66:**3608–3615.
21. **Imachi, H., Y. Sekiguchi, Y. Kamagata, A. Ohashi, and H. Harada.** 2002.

Pelotomaculum thermopropionicum gen. nov., sp. nov., an anaerobic, thermophilic, syntrophic propionate-oxidizing bacterium. Int. J. Syst. Evol. Microbiol. **52:**1729–1735.
22. **Jackson, B. E., and M. J. McInerney.** 2002. Anaerobic microbial metabolism can proceed close to thermodynamic limits. Nature **415:**454–456.
23. **Kanehisa, M., and S. Goto.** 2000. KEGG: Kyoto Encyclopedia of Genes and Genomes. Nucleic Acids Res. **28:**27–30.
24. **Katayama, H., T. Nagasu, and Y. Oda.** 2001. Improvement of in-gel digestion protocol for peptide mass fingerprinting by matrix-assisted laser desorption/ionization time-of-flight mass spectrometry. Rapid Commun. Mass Spectrom. **15:**1416–1421.
25. **Kneller, D. G., F. E. Cohen, and R. Langridge.** 1990. Improvements in protein secondary structure prediction by an enhanced neural network. J. Mol. Biol. **214:**171–182.
26. **Larimer, F. W., P. Chain, L. Hauser, J. Lamerdin, S. Malfatti, L. Do, M. L. Land, D. A. Pelletier, J. T. Beatty, A. S. Lang, F. R. Tabita, J. L. Gibson, T. E. Hanson, C. Bobst, J. L. T. Torres, C. Peres, F. H. Harrison, J. Gibson, and C. S. Harwood.** 2004. The genome sequence of the metabolically versatile photosynthetic bacterium *Rhodopseudomonas palustris*. Nat. Biotechnol. **22:**55–61.
27. **Liu, Y., D. L. Balkwill, H. C. Aldrich, G. R. Drake, and D. R. Boone.** 1999. Characterization of the anaerobic propionate-degrading syntrophs *Smithella propionica* gen. nov., sp. nov. and *Syntrophobacter wolinii*. Int. J. Syst. Bacteriol. **49:**545–556.
28. **Makita, Y., M. Nakao, N. Ogasawara, and K. Nakai.** 2004. DBTBS: database of transcriptional regulation in *Bacillus subtilis* and its contribution to comparative genomics. Nucleic Acids Res. **32:**D75–D77.
29. **Marmur, J.** 1961. A procedure for the isolation of deoxyribonucleic acid from microorganisms. J. Mol. Biol. **3:**208–218.
30. **Nölling, J., G. Breton, M. V. Omelchenko, K. S. Makarova, Q. Zeng, R. Gibson, H. M. Lee, J. Dubois, D. Qiu, J. Hitti, Y. I. Wolf, R. L. Tatusov, F. Sabathe, L. Doucette-Stamm, P. Soucaille, M. J. Daly, G. N. Bennett, E. V. Koonin, and D. R. Smith.** 2001. Genome sequence and comparative analysis of the solvent-producing bacterium *Clostridium acetobutylicum*. J. Bacteriol. **183:**4823–4838.
31. **Omerchenko, M. V., K. S. Makarova, Y. I. Wolf, I. B. Rogozin, and E. V. Koonin.** 2003. Evolution of mosaic operons by horizontal gene transfer and gene displacement in situ. Genome Biol. **4:**R55.
32. **Page, R. D. M.** 1996. TREEVIEW: an application to display phylogenetic trees on personal computers. Comput. Appl. Biosci. **12:**357–358.
33. **Plugge, C. M., C. Dijkema, and A. J. M. Stams.** 1993. Acetyl-CoA cleavage pathway in a syntrophic propionate oxidizing bacterium grown on fumarate in the absence of methanogens. FEMS Microbiol. Lett. **110:**71–76.
34. **Plugge, C. M., M. Balk, and A. J. M. Stams.** 2002. *Desulfotomaculum thermobenzoicum* subsp. *thermosyntrophicum* subsp. nov., a thermophilic, syntrophic, propionate-oxidizing, spore-forming bacterium. Int. J. Syst. Evol. Microbiol. **52:**391–399.
35. **Price, M. N., K. H. Huang, A. P. Arkin, and E. J. Alm.** 2005. Operon formation is driven by co-regulation and not by horizontal gene transfer. Genome Res. **15:**809–819.
36. **Saitou, N., and M. Nei.** 1987. The neighbor-joining method: a new method for reconstructing phylogenetic trees. Mol. Biol. Evol. **4:**406–425.
37. **Sambrook, J., E. F. Fritsch, and T. Maniatis.** 1989. Molecular cloning: a laboratory manual, 2nd ed. Cold Spring Harbor Laboratory, Cold Spring Harbor, N.Y.
38. **Schink, B.** 1985. Mechanism and kinetics of succinate and propionate degradation in anoxic freshwater sediments and sewage sludge. J. Gen. Microbiol. **131:**643–650.
39. **Schink, B.** 1997. Energetics of syntrophic cooperation in methanogenic degradation. Microbiol. Mol. Biol. Rev. **61:**262–280.
40. **Siebers, B., B. Tjaden, K. Michalke, C. Dörr, H. Ahmed, M. Zaparty, P. Gordon, C. W. Sensen, A. Zibat, H. P. Klenk, S. C. Schuster, and R. Hensel.** 2004. Reconstruction of the central carbohydrate metabolism of *Thermoproteus tenax* by use of genomic and biochemical data. J. Bacteriol. **186:**2179–2194.
41. **Smith, D. R., L. A. Doucette-Stamm, C. Deloughery, H. Lee, J. Dubois, T. Aldredge, R. Bashirzadeh, D. Blakely, R. Cook, K. Gilbert, D. Harrison, L. Hoang, P. Keagle, W. Lumm, B. Pothier, D. Qiu, R. Spadafora, R. Vicaire, Y. Wang, J. Wierzbowski, R. Gibson, N. Jiwani, A. Caruso, D. Bush, and J. N. Reeve.** 1997. Complete genome sequence of *Methanobacterium thermoautotrophicum* ΔH: functional analysis and comparative genomics. J. Bacteriol. **179:**7135–7155.
42. **Tatusov, R. L., N. D. Fedorova, J. D. Jackson, A. R. Jacobs, B. Kiryutin, E. V. Koonin, D. M. Krylov, R. Mazumder, S. L. Mekhedov, A. N. Nikolskaya, B. S. Rao, S. Smirnov, A. V. Sverdlov, S. Vasudevan, Y. I. Wolf, J. J. Yin, and D. A. Natale.** 2003. The COG database: an updated version includes eukaryotes. BMC Bioinformatics **4:**41.
43. **Taylor, B. L., and I. B. Zhulin.** 1999. PAS domains: internal sensors of oxygen, redox potential, and light. Microbiol. Mol. Biol. Rev. **63:**479–506.
44. **Thauer, R. K., K. Jungermann, and K. Decker.** 1977. Energy conservation in chemotrophic anaerobic bacteria. Bacteriol. Rev. **41:**100–180.
45. **Thompson, J. D., T. J. Gibson, F. Plewniak, F. Jeanmougin, and D. G. Higgins.** 1997. The ClustalX windows interface: flexible strategies for multiple sequence alignment aided by quality analysis tools. Nucleic Acids Res. **24:**4876–4882.
46. **Van Kuijk, B. L., E. Schlosser, and A. J. Stams.** 1998. Investigation of the fumarate metabolism of the syntrophic propionate-oxidizing bacterium strain MPOB. Arch. Microbiol. **169:**346–352.
47. **Wallrabenstein, C., E. Hauschild, and B. Schink.** 1995. *Syntrophobacter pfennigii* sp. nov., new syntrophically propionate-oxidizing anaerobe growing in pure culture with propionate and sulfate. Arch. Microbiol. **164:**346–352.
48. **Wang, L. F., and R. H. Doi.** 1986. Nucleotide sequence and organization of *Bacillus subtilis* RNA polymerase major sigma (sigma 43) operon. Nucleic Acids Res. **14:**4293–4307.
49. **Zhang, J., and T. L. Madden.** 1997. PowerBLAST: a new network BLAST application for interactive or automated sequence analysis and annotation. Genome Res. **7:**649–656.